Regulation of Cargo-Selective Endocytosis by Dynamin 2 GTPase-Activating Protein Girdin

Liang Weng, et al.

Supplementary Materials and Methods

Antibodies. The antibodies used in this study were as follows: sheep anti-girdin antibody (R&D Systems, Minneapolis, MN, #AF5345, for WB and IP), rabbit anti-girdin antibody (IBL, Gumma, Japan, for immunofluorescence (IF)), anti-clathrin HC antibody (clone TD.1, Santa Cruz Biotechnology, Santa Cruz, CA, for WB and clone X22, Abcam, Cambridge, MA, for IF), mouse anti-transferrin receptor antibody (clone H68.4, Invitrogen, Carlsbad, CA, for WB and ELISA), rabbit anti-transferrin receptor antibody (Santa Cruz Biotechnology, #sc-9099, for IP), anti-E-cadherin antibody (clone HECD-1, Takara, Osaka, Japan, for IF and IP and clone 36/E-cadherin, BD Biosciences, San Jose, CA, #610182, for ELISA and WB), anti-α5 integrin antibody (clone VC5, BD Biosciences, #555651, for ELISA), anti-EGFR antibody (clone 13G8, Santa Cruz Biotechnology, for WB and clone 528, Santa Cruz Biotechnology, for IP and IF), anti-EGFR1 antibody (BD Biosciences, #610467, for ELISA), anti-β1 integrin antibody (clone P5D2, Santa Cruz Biotechnology, for IF and IP and clone 18/CD29, BD Biosciences, #610467, for WB), anti-dynamin I/II (clone 41, BD Biosciences, #610246), anti-dynamin 2 (Santa Cruz Biotechnology, #sc-166526), anti-GST antibody (Santa Cruz Biotechnology, #sc-459), anti-Myc antibody (clone 9E10, Santa Cruz Biotechnology), anti-AP2 antibody (clone AP6, Abcam, for IF), anti-Adaptin α antibody (clone 8, BD Biosciences, #610501, for WB; Santa Cruz Biotechnology, sc-17771, for IP), anti-Adaptin β antibody (clone 74, BD Biosciences, #610381), anti-Adaptin γ antibody (clone 88, BD Biosciences, #610385), anti-Adaptin σ antibody (clone 18, BD Biosciences, #611328), rabbit anti-GFP antibody (MBL, Nagoya, Japan, #598), anti-poly histidine antibody (clone HIS-1, Sigma, St. Louis, MO), anti-Flag antibody (clone M2, Sigma), anti-β-actin antibody

(clone AC-74, Sigma), normal mouse IgG (Millipore, Milford, MA, #12-371), normal rabbit IgG (Millipore, #12-370), and normal sheep IgG (Millipore, #12-515).

Retrovirus infection. To generate HeLa cells stably expressing E-cadherin, 24 μg of pRetroQ-E-cadherin and 4 μg of pVSV-G (vesicular stomatitis virus G protein) vector (Clontech) were co-transfected into GP2-293 packaging cells (Clontech). Twenty-four hr after the transfection, the medium was replaced with 5 mL of fresh DMEM containing 10% FBS, and the cells were further cultured at 32°C to facilitate virus production. HeLa cells were infected with virus-containing supernatants harvested 48 hr post-transfection, followed by selection with 2 μg/mL puromycin.

Protein expression and purification. For the purification of GST fusion proteins, BL21 competent cells (Stratagene) transformed with the indicated plasmid were cultured in 2x YT medium containing 100 μg/mL of ampicillin at 37°C until the absorbance at 600 nm wavelength (A600) reached 0.6 - 0.8. Protein expression was induced by adding 100 μM isopropyl beta-D-thiogalactoside (IPTG), followed by continuous culture at 25°C for an additional 4 hr. The cell pellets were suspended in homogenizing buffer (20 mM Tris-HCl, pH 8.0, 1 mM EDTA, 1 mM DTT, 10% sucrose) supplemented with complete protease inhibitor cocktail (Roche) and sonicated extensively. The lysates were then cleared via centrifugation at 37,000 rpm for 1 hr and applied to a column of glutathione-Sepharose 4B beads with a 1-mL bed volume (GE Healthcare) equilibrated with 20 mL of TED buffer (20 mM Tris-HCl, 1 mM EDTA, 1 mM DTT, pH 8.0). The column was washed extensively with 10 mL of TED buffer, and the GST fusion protein was eluted using elution buffer (10 mM glutathione in TED buffer), followed by dialysis with TED buffer.

For the purification of proteins tagged with histidine residues, Rosseta (DE3)-competent cells (Stratagene) transformed with the indicated plasmid were cultured in 2x YT medium containing 100 μg/mL of ampicillin at 37°C until the A600 reached 0.5 - 0.6. 300 μM IPTG was then added to induce the expression of

recombinant proteins, followed by additional culture at 37°C for 3 hr. The cell pellets were suspended in buffer A (50 mM NaH_2PO_4, 300 mM NaCl, 10 mM imidazole, pH 8.0) supplemented with complete protease inhibitor cocktail, sonicated extensively, and then centrifuged. The supernatant was applied to a column of TALON metal affinity resin (Clontech) with a 1 mL of bed volume equilibrated with 20 mL of buffer A. The column was then washed using 20 mL of buffer B (50 mM NaH_2PO_4, 300 mM NaCl, 20 mM imidazole, pH 8.0), and the proteins were eluted using the elution buffer (20 mM NaH_2PO_4, 300 mM NaCl, 250 mM imidazole, pH 8.0). For histidine-tagged proteins used for the in vitro binding assays, the eluate was dialyzed against Tris-buffered saline (TBS) using a 10-kDa cutoff membrane (Slide-A-Lyzer G2 Dialysis Cassettes, Thermo Scientific, Waltham, MA). To prepare recombinant histidine-tagged dynamin 2 for dynamin GTPase activity assays, the eluate was further purified on an anion exchange column (HiTrapQ HP, GE Healthcare) using the ÄKTAprime Plus liquid chromatography system (GE Healthcare) according to the manufacturer's instructions. Purified dynamin proteins were dialyzed against a dialysis buffer (20 mM HEPES-KOH, 150 mM KCl, 1 mM EDTA, 1 mM EGTA, 0.5 mM DTT, pH 7.5). The concentration of recombinant protein was determined by using the Qubit Protein Assay kits and Qubit fluorometer (Invitrogen).

Immunoprecipitation and Western blot analysis. The HeLa cells or COS7 cells were lysed in IP lysis buffer (25 mM Tris-HCl, 150 mM NaCl, 1% NP-40, 1 mM EDTA, 5% glycerol, pH 7.4) supplemented with complete Mini protease inhibitor and PhosSTOP phosphatase inhibitor cocktails (Roche). The lysates were cleared via centrifugation at 12,000 x g for 15 min, and the supernatants were incubated with 5 µg of the appropriate primary antibodies or normal immunoglobulin G (IgG) on a rotator at 4°C for 3 hr, followed by the addition of 40 µL of protein A or G Sepharose beads (Sigma) at 4°C for 3 hr. The beads were then washed three times with IP lysis buffer, and the protein complex was eluted using 100 µL of 1x SDS sample buffer. For the detection of endogenous girdin/dynamin interaction, HeLa cells were lysed

with GTPase IP buffer (20 mM Tris-HCl, 120 mM NaCl, 1 mM EDTA, 0.8% Triton X-100, 5 mM $MgCl_2$, pH 7.4) and centrifuged, followed by adding 7.5 μL of 0.5 M EDTA (pH 8.0) to each 500 μL of lysate to chelate all of Mg^{2+} with excess EDTA. Then, 5 μL of 0.5 M GTPγS or GDP (final concentration, 0.5 mM) was added to the lysate, followed by incubation for 15 minutes at room temperature to load GTPγS or GDP. Next, 30 μL of 1 M $MgCl_2$ was added to the lysate to stabilize the binding of the nucleotide to the dynamin GTPase. Finally, 2 μg of each antibody was added to the lysate and incubated for 3 hr, followed by precipitation by protein G bead, and the precipitated protein complex was eluted with SDS sample buffer.

The samples were separated using sodium dodecyl sulfate polyacrylamide gel electrophoresis (SDS-PAGE). The proteins were transferred onto polyvinylidene difluoride (PVDF) membranes, blocked with 5% skimmed milk in PBS-T (PBS containing 0.1% Tween 20), incubated with primary antibodies and detected by using horseradish peroxidase-conjugated antibodies (Dako, Carpinteria, CA). During Western blot analysis for detecting girdin, the primary antibody was diluted in Can-Get-Signal solution 1 (Toyobo, Osaka, Japan) to enhance antibody-antigen binding. In Co-IP experiments to test the interaction between girdin and cargoes (Figure 4B and 4C), we used antibodies that recognize the extracellular domain of each cargo to exclude the possibility that the girdin binding sites of cargoes overlap with the epitope for the antibodies used.

Gel filtration. Three dishes (100 mm diameter dish) of confluent HeLa cells were washed with cold PBS and suspended in 1 mL of gel filtration buffer (25 mm Tris/HCl, pH 8.0, 250 mm NaCl, 1 mm DTT) supplemented with complete Mini protease inhibitor and PhosSTOP phosphatase inhibitor cocktails (Roche).The suspension was sonicated and centrifuged at 12, 000 g for 15 min at 4°C. The supernatants were passed through 0.45μm filter unit (Millipore) and then adjusted to a total protein concentration of 2 mg/mL. 0.5 mL of cell lysate was applied to a Superose 6 10/300 GL column equilibrated with gel filtration buffer using the ÄKTAprime Plus liquid

chromatography system (GE Healthcare).The elution was performed with the same buffer at a flow rate of 0.2 mL/min. Fractions of 0.5 mL were collected. The column was calibrated with protein standards (thyroglobulin, 669 kDa; ferritin, 440 kDa; catalase, 232 kDa; aldolase, 158kDa, Amersham Biosciences).

In vitro binding assays. 50 pmol of purified recombinant GST fusion proteins (baits) rebound to 50 µL of glutathione-Sepharose 4B beads in TED buffer were mixed with 300 pmol of purified recombinant prey proteins or cell lysates prepared from 10 mL of bacterial culture expressing prey proteins. After the incubation at 4°C for 2 to 3 hr, the beads were washed three times using TED buffer. The bound proteins were eluted using 1x SDS sample buffer, separated by SDS-PAGE, and then subjected to CBB staining or Western blot analysis. For the detection of direct girdin/dynamin interaction, we used GTPase IP buffer (20 mM Tris-HCl, 120 mM NaCl, 1 mM EDTA, 0.8% Triton X-100, 5 mM $MgCl_2$, pH7.4) to dilute purified dynamin 2, which were then loaded with either GTPγS or GDP, followed by the incubation with 50 pmol of purified recombinant GST fusion proteins bound to 50 µL of glutathione-sepharose 4B beads for 2 hr.

Electron Microscopy. For transmission EM, cells were fixed with 4% paraformaldehyde (PFA) and 2% glutaraldehyde in 0.1M phosphate buffer for 30 min at 4°C, washed in the phosphate buffer, postfixed with 2% osmium tetroxide in the phosphate buffer for 30 min at 4°C, dehydrated with ethanols and embedded in Epon. Ultrathin sections were counterstained with uranyl acetate and lead citrate and analyzed by an electron microscope (JEM-1400EX; JEOL). For the quantification of the morphology of CCPs, the images were taken blindly by an experienced technician, who was shielded from the projects in the study. She took the images of all of CCPs available in each field without arbitrarily excluding any of them. We then independently analyzed the morphology of all of the CCPs images for the quantification. For immune-EM, HeLa cells were stimulated with 2 ng/ml EGF for 10 min, then the cells were fixed for 30 min in 4% PFA and 0.5% glutaraldehyde in

0.1M phosphate buffer at 4°C, dehydrated and embedded in LR White Resin (London Resin Company Ltd., Berkshire, England). After blocking with 1% BSA in PBS, ultrathin sections were incubated with anti-TfR or EGFR antibodies overnight at 4°C, washed three times in PBS, incubated with 10 nm gold-conjugated secondary antibodies (Sigma-aldrich Co., USA) for 2 hr at room temperature, washed with PBS for three times, fixed in 2% glutaraldehyde in the phosphate buffer, rinsed in water, air-dried and finally weakly stained with uranyl acetate.

Immunofluorescence studies and time-lapse recordings with the TIRF microscope. Immunofluorescence studies were performed as previously described (Enomoto et al., 2005). Cells were plated on glass base dishes, fixed, and stained with the indicated antibodies. The cells were imaged using a confocal laser-scanning microscope (Fluoview FV500, Olympus, Tokyo, Japan) or total internal reflection fluorescence (TIRF) system on a Nikon A1Rsi microscope equipped with 60x or 100x (1.49NA) TIRF objectives (Nikon, Tokyo, Japan) and a high-sensitivity electron-multiplying charged-coupled device (EMCCD) camera (Andor, Tokyo, Japan). For time-lapse recording experiments, the cells were seeded on 3.5 cm glass base dishes in DMEM without phenol red (Sigma), supplemented with 10% FBS, and placed on a stage heated to 37°C. Live-cell imaging data were acquired using the TIRF system equipped with 100x Apo TIRF objectives under the control of NIS-Elements software (Nikon). The kymograph of clathrin-coated pits was generated with NIS-Elements software.

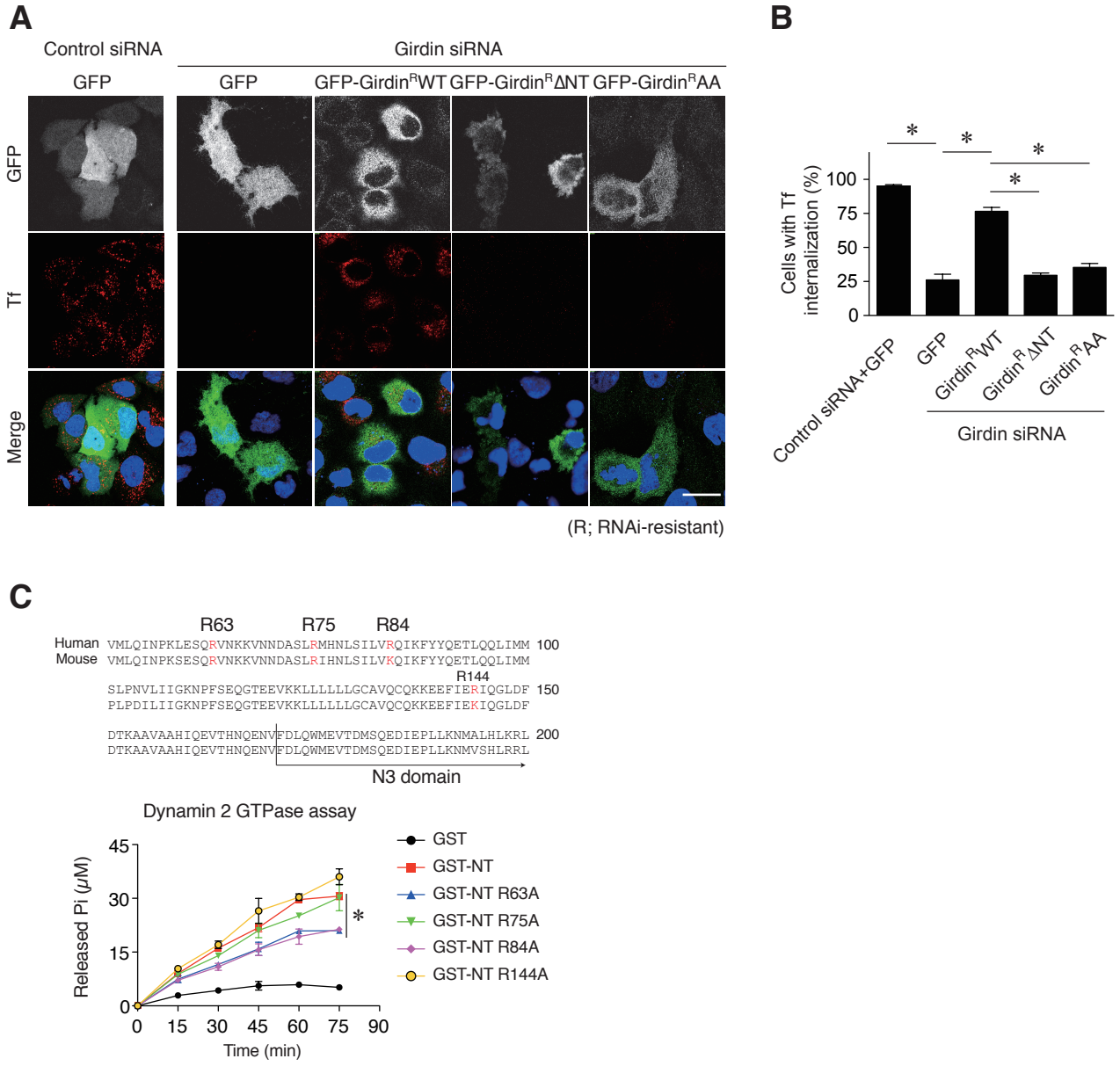

Supplementary Figure S1. Weng et al.

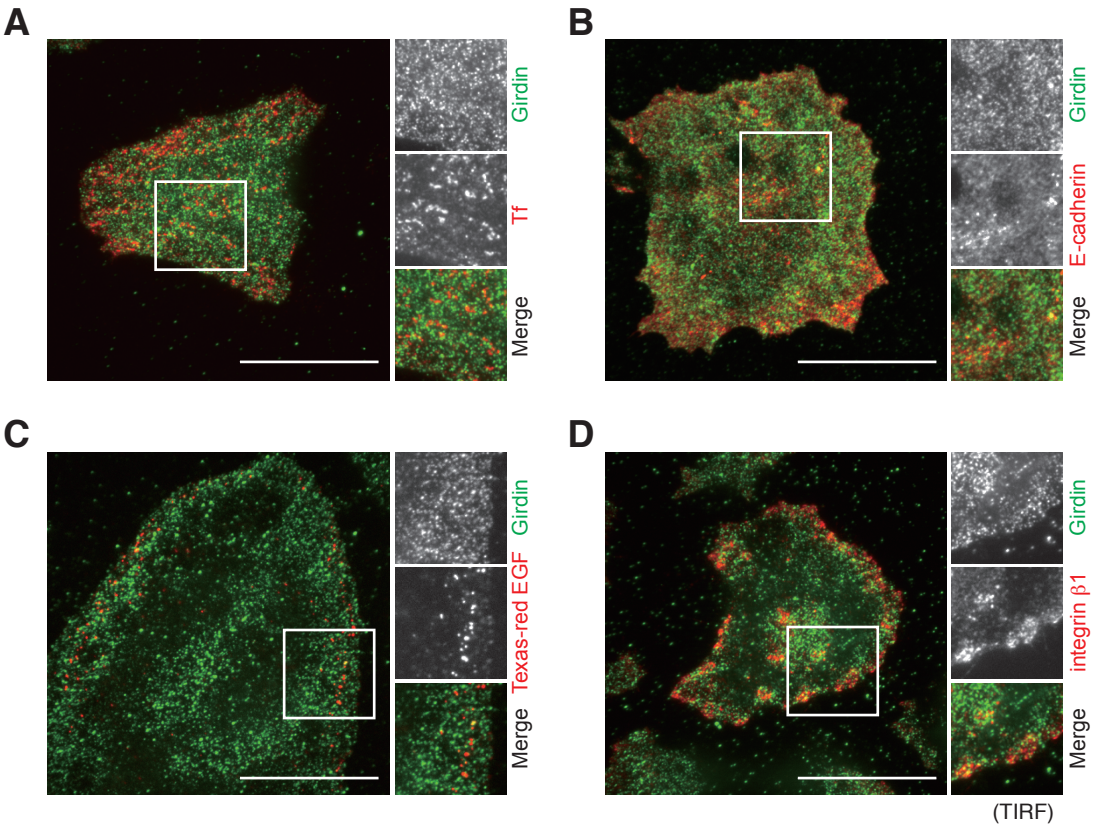

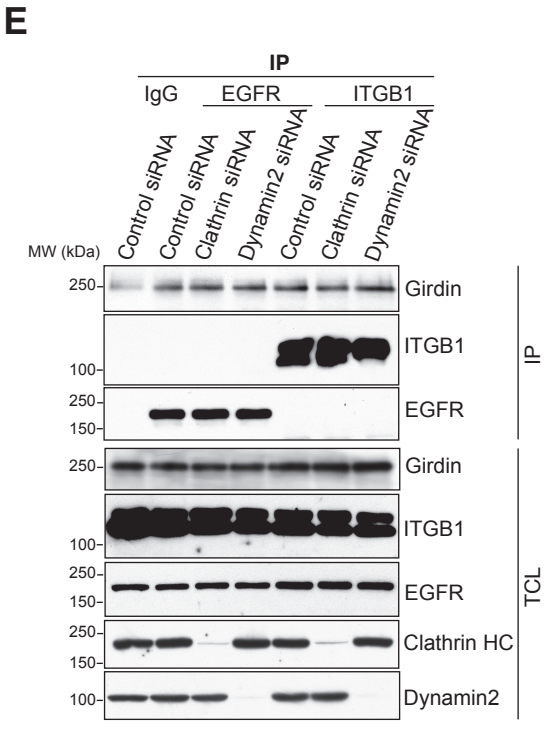

Supplementary Figure S2. Weng et al.

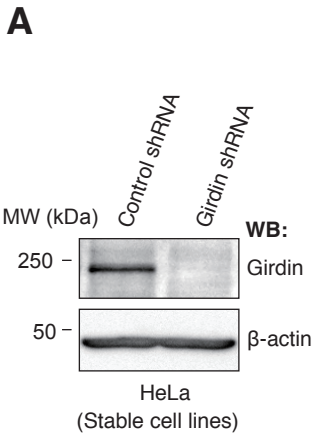

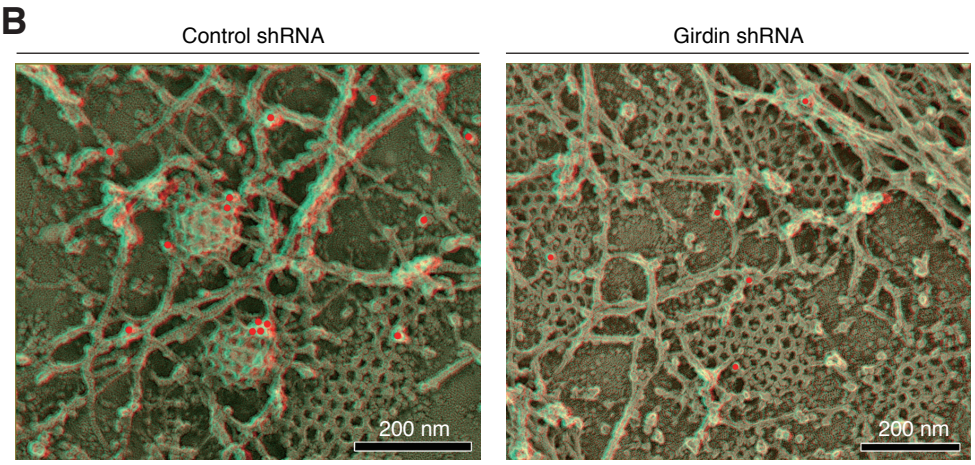

C

	CCP morphology	Total number of counted CCPs	Number of CCPs with immunogold labeling	Number of immunogold labeling per each CCP
Control shRNA	Mature CCP	58	53	4.8
	Undergoing scission	42	26	1.86
Girdin shRNA	Mature CCP	55	36	1.3
	Undergoing scission	17	3	0.18

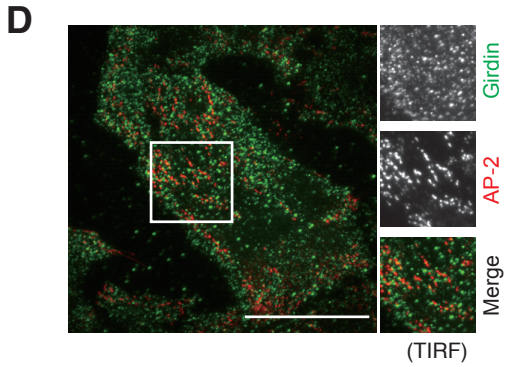

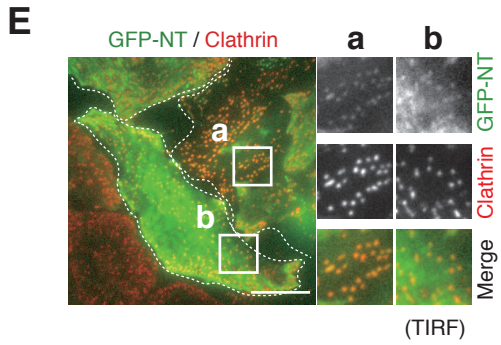

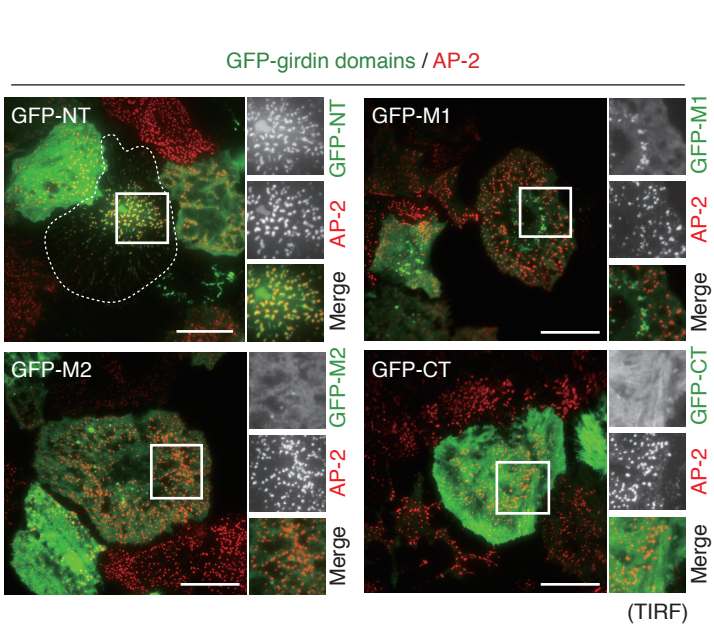

Supplementary Figure S3.
Weng et al.

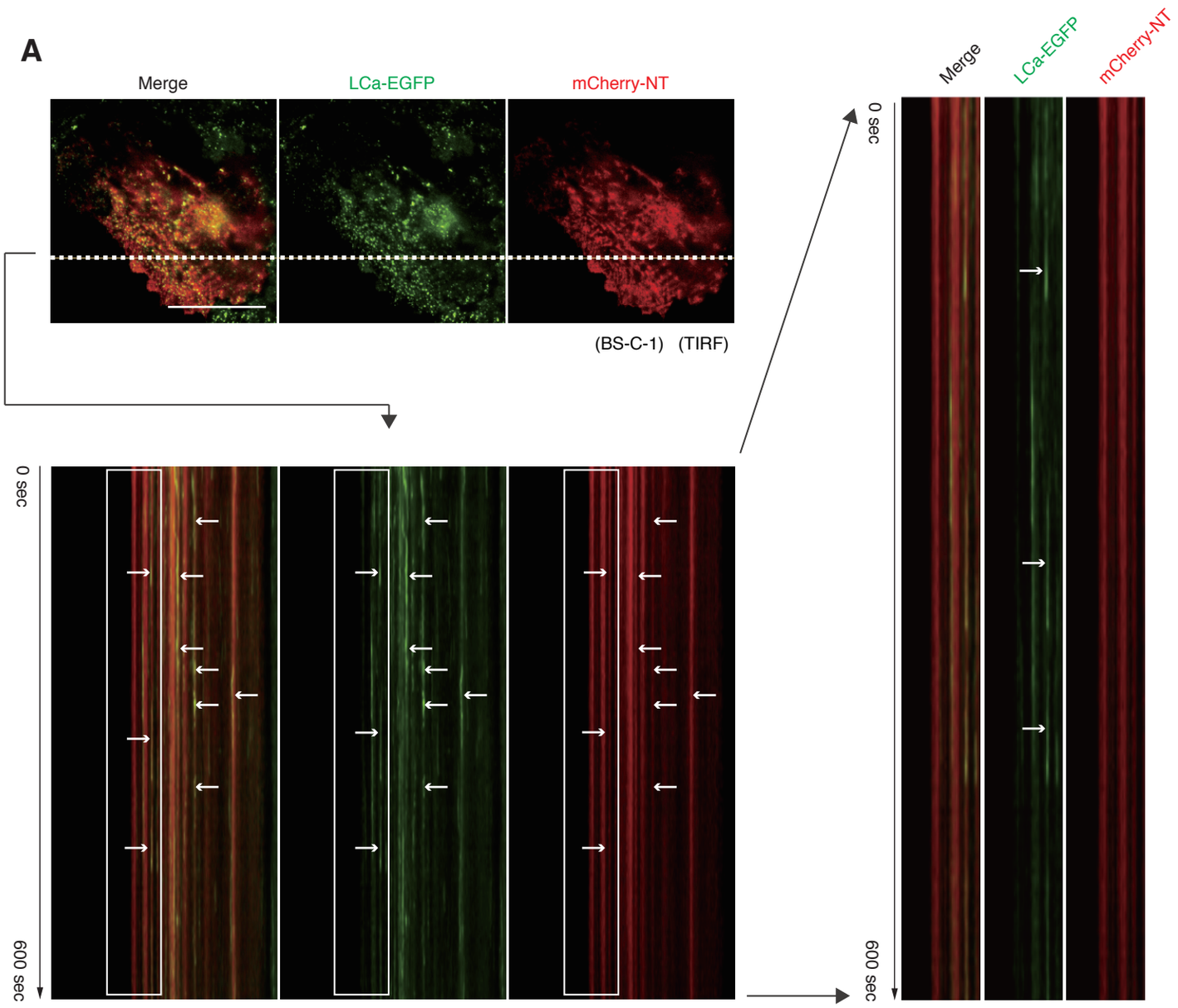

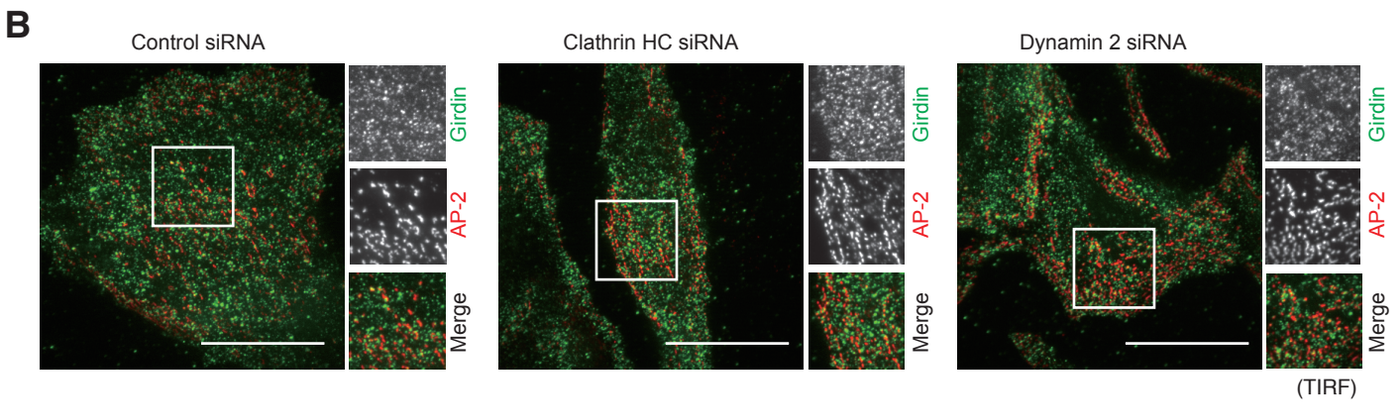

Supplementary Figure S4. Weng et al.

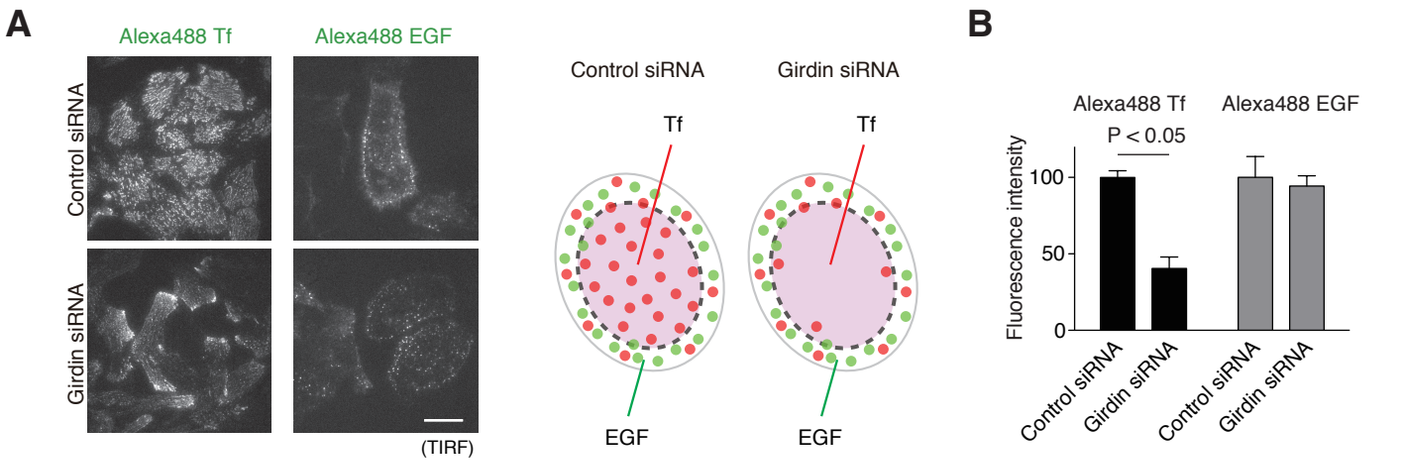

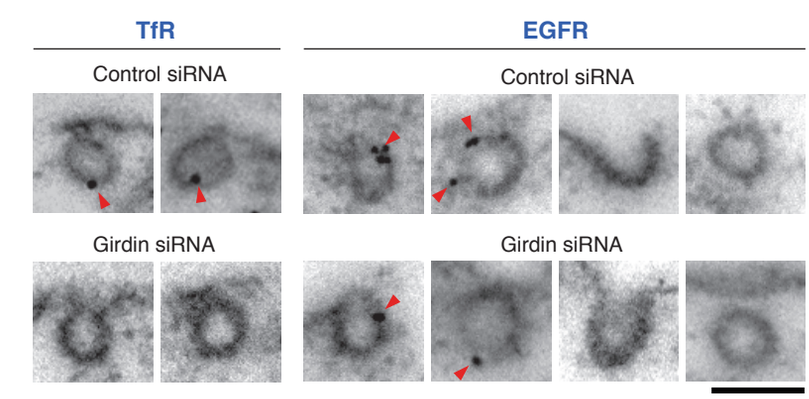

D

TfR

	Control siRNA	Girdin siRNA
TfR-positive CCVs	30	10
Number of counted CCVs	62	72
Positivity (%)	48.4	13.9

EGFR

	Control siRNA	Girdin siRNA
EGFR-positive CCVs	17	18
Number of counted CCVs	74	85
Positivity (%)	23.0	21.2

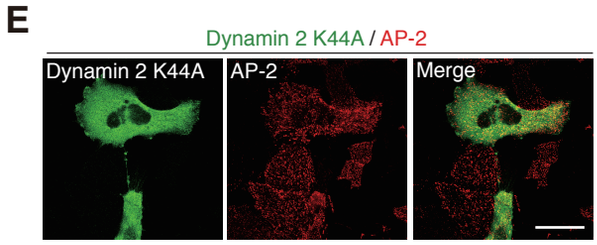

Supplementary Figure S5. Weng et al.

Legends for Supplementary Figures

Supplementary Figure S1. Girdin regulates endocytosis as a GAP for dynamin 2.

(A, B) HeLa cells were transfected with the indicated combinations of control and girdin siRNA and RNAi-resistant version (Enomoto et al., 2005) of GFP-girdin WT (wild-type), ΔN (deleted of the NT domain), and AA (R63 and R84 are replaced with alanines), followed by Tf internalization assays. Quantification of Tf internalization in the experiments shown in **(B)**. The percentage of cells with internalized Tf in each group (100 cells from three independent experiments) was quantified. Data are presented as means ± SE (n=3). Scale bar, 20 μm.

(C) An important role of arginines in the girdin NT domain in its GAP activity toward dynamin 2. Shown in the upper panel is the sequence of the NT domain of human girdin aligned with mouse girdin. Arginines, which were predicted to be important for the GAP activity by reference to the findings on structure-function relationship of Ras GAP proteins, are shown in red. In the experiments shown in lower panel, purified girdin NT proteins with the indicated mutation were subjected to dynamin 2 GTPase activity assays. The asterisks indicate statistical significance compared with GST-NT ($P < 0.05$). Data are presented as means ± SE (n = 3).

Supplementary Figure S2. Girdin colocalizes with the endocytic sites for the cargoes.

(A-D) Colocalization between girdin and endocytic sites for the indicated cargoes was investigated using TIRF microscopy according to the methods described in the Method section. Endogenous girdin shows partial colocalization with the endocytic sites for the four cargoes. Scale bar, 20 μm.

(E) Total cell lysates from HeLa cells transfected with the indicated siRNA were subjected to immunoprecipitation by IgG, EGFR or integrin β1 antibodies, followed

by Western blot analysis. Knockdown of clathrin heavy chain or dynamin 2 has no apparent effect on the interaction between girdin and EGFR or integrin β1.

Supplementary Figure S3. Localization of girdin on CCPs through its NT domain.

(A) Western blot evaluation of the knockdown efficiency by girdin shRNA in HeLa cells subjected to deep-etch electron microscopic analysis.

(B, C) Localization of girdin on CCPs examined by quick-freeze deep-etch electron microscopy of unroofed cells. Representative images of immunogold labeling for girdin molecules on CCPs and those undergoing scission, which exhibited a clear dot surrounded by a halo of platinum-carbon coating (pseudo-colored red), are shown. The labeling efficiency (the percentage of cells with the immunogold labeling) and the number of labels per CCP in control and girdin knockdown cells are evaluated in **(C)**. The data indicated the specificity of the immunolabeling to detect girdin molecules. Scale bar, 200 nm.

(D) Colocalization of girdin with the CCPs marker AP-2 in HeLa cells under observation using TIRF microscopy. The region within the box is shown at a higher magnification in the adjacent panels. Scale bar, 20 μm.

(E) Colocalization of the girdin NT domain with clathrin HC in HeLa cells under observation using TIRF microscopy. The regions within the boxes (a and b) are shown at a higher magnification in the adjacent panels. Dotted lines delineate the contours of the girdin NT-transfected cells, scale bar, 20μm.

(F) GFP-NT, but none of the other girdin domains (M1, M2 and CT) colocalized with CCPs in HeLa cells under observation using TIRF microscopy. The regions within the boxes are shown at a higher magnification in the adjacent panels. Scale bar, 20 μm.

Supplementary Figure S4. Involvement of girdin from the early to late stages of CCP formation.

(A) BS-C-1 cells stably expressing clathrin light chain A (LCa)-GFP (green) were transfected with mCherry-NT (red), the formation of CCPs was observed by TIRF microscope (upper left panel). A kymograph was produced from a transverse slice (indicated by a dotted line) across the cell (lower left panel). In the kymograph, CCPs (arrows) preferentially formed at the sites containing mCherry-NT within the observed time interval. The regions within the boxes in the kymograph are shown in the right panels at a higher magnification. The data showed that mCherry-NT was constitutively located within the regions (arrows) where CCPs were preferentially and repeatedly formed, suggesting that the girdin NT domain was involved in the formation of CCPs. A Video of the observed cell is available in Supplementary Video S1. Scale bar, 20 μm.

(B) Localization of girdin was observed in HeLa cells transfected with the indicated siRNA by TIRF microscopy. The results indicate that the knockdown of clathrin or dynamin 2 has no effect on the colocalization between girdin and AP-2.

Supplementary Figure S5. Girdin is involved in CCP formation in the center of cells independently of dynamin function.

(A, B) The endocytic sites of Tf and EGF were observed by TIRF microscopy in control and girdin knockdown HeLa cells. Shown in the right panel is the illustration indicating the endocytic sites for each cargo. The fluorescence of each cargo per cell was quantified in **(B)**. The values in control cells are presented as 100%. Statistical significance compared with control is indicated. Data are presented as means ± SE (n = 50).

(C, D) Immunoelectron microscopic analysis of TfR and EGFR on clathrin-coated vesicles (CCVs) in control and girdin knockdown HeLa cells. Representative images of immunogold labeling for TfR (left panel) and EGFR (right panel) and quantitative analysis **(D)** are shown. Arrowheads denote the TfR and EGFR immunogold labeling on CCVs. The scale bar is 250 nm.

(E) The effect of dynamin on CCPs formation was checked in HeLa cells. Cells transfected with dynamin K44A mutant showed normal CCPs formation as observed for non-transfected cells. Scale bar, 20 μm.